# Kinetic parameters for OH nightglow modeling consistent with recent laboratory measurements

Steven Adler-Golden
Spectral Sciences Inc., Burlington, Massachusetts

**Abstract.** An improved kinetic model for the Meinel bands of OH has been constructed from rate constants and Einstein A coefficients derived in recent laboratory experiments. Using a semiempirical parameterization of the state-to-state rate constants for OH(v) quenching by $O_2$, the absolute OH(v) nightglow radiances are modeled to within the accuracies of the atmospheric constituent concentrations and the radiometric calibrations. Collisional quenching is found to be predominantly multiquantum at high v but single-quantum at low v.

## 1. Introduction

The visible nightglow spectrum is dominated by the Meinel (vibrational) bands of the hydroxyl (OH) radical, which are generated in the mesopause region from the H + $O_3$ reaction. The usefulness of this emission for atmospheric remote sensing, as well as the desire to explain recent observations of nonthermal rotational state distributions [*Pendleton et al*., 1989; *Smith et al.*, 1992; *Dodd et al.*, 1994] provide strong motivations for improving our understanding of OH(v) kinetics. Applications include deriving O and H atom profiles [*Thomas*, 1990; *McDade and Llewelyn*, 1987; *Takahashi et al*., 1996] and studying gravity wave and other atmospheric fluctuations [*Tarasick and Shepherd*, 1992; *Makhlouf et al*., 1995].

Significant advances in modeling the Meinel bands have been made in recent years with new laboratory experiments that have led to more reliable Einstein A coefficients for emission [*Nelson et al*., 1990; *Holtzclaw et al*., 1993] and rate constants for net OH(v) removal by $O_2$ and $N_2$ at room temperature [*Knutsen et al*., 1996; *Chalamala and Copeland*, 1993; *Dodd et al*., 1991]. A limited investigation of the temperature dependence of OH(v) relaxation by $O_2$ has recently been conducted (M. J. Dyer et al. unpublished data, 1997). However, these data by themselves do not provide sufficiently detailed information (i.e., a complete set of state-to-state relaxation rate constants at mesospheric temperatures) for accurately modeling the altitude profiles of all OH(v) states. Prior to this work, several kinetic models were developed using primarily atmospheric data and making various simplified assumptions about the vibrational relaxation pathway [e.g., *McDade et al*., 1987; *McDade and Llewelyn*, 1987]. These models have shown considerable empirical success, but they do not provide either unambiguous OH(v) profile predictions or complete consistency with the laboratory measurements.

While it is clear that further measurements are ultimately needed, modeling which makes better and more complete use of existing information can considerably improve our knowledge of OH(v) kinetics. In particular, by requiring consistency between laboratory and atmospheric measurements a much more realistic description of the vibrational relaxation process can be obtained. In the current investigation, a semiempirical state-to-state model motivated by molecular dynamics simulations was developed and parameterized using a variety of data. Atmospheric simulations using this model provide a complete, quantitative description of OH(v) altitude profiles and absolute nightglow radiances.

As has been discussed by several authors [*McDade*, 1991; *Shalashilin et al.*, 1995; *Knutsen et al*., 1996], there is strong evidence that OH(v) relaxation by the dominant quencher, $O_2$, is multiquantum at high v but primarily single quantum at low v. *McDade et al*. [1987] and *McDade and Llewelyn* [1987] used average OH(v) zenith radiances and an altitude profile of (8 - 3) band emission measured in the ETON experiment to extract quenching parameters for two limiting vibrational relaxation assumptions: (1) "sudden death," in which OH(v) is either chemically removed or multiquantum-quenched to OH(0), and (2) "cascade" (single-quantum) relaxation from OH(v) to OH(v-1). Both the v dependence and the absolute magnitudes of the "sudden death" model rate constants are in rough agreement with recent laboratory measurements on $O_2$, the major atmospheric quencher, for high-v states [*Knutsen et al*., 1996], whereas the results from the "cascade" model are incompatible with the laboratory data. Multiquantum quenching is further supported by the laser-induced fluorescence experiments of *Chalamala and Copeland* [1993], who reported little or no increase in the OH population in v=6 relative to that in v=9 when $O_2$ was added to their flow system. The low-v states of OH have been studied by *Dodd et al*. [1991] in a pulsed-discharge system. They concluded that at least for v=1-3 the vibrational relaxation by $O_2$ is mainly, and perhaps entirely, single quantum.

In the current work, the OH(v) relaxation by $O_2$ is handled using a simple expression for the state-to-state rate constant matrix that contains a free parameter controlling both the degree and the v dependence of multiquantum relaxation. The parameter value is determined by matching observed relative, rather than absolute, OH(v) radiances, making it nearly independent of Einstein coefficient uncertainties and reducing the sensitivity to atmospheric species and temperature profiles. A temperature-scaling factor, which turns out to be close to unity, is included in the rate constant expression in order to match the shape of the (8 - 3) band profile measured in ETON. The results of the present study indicate that the collisional relaxation of OH(v) in the atmosphere proceeds from single quantum at low v to almost entirely multiquantum at v = 7 to 9.

In the following sections, the kinetic mechanism is summarized, nightglow data are simulated to fix the relaxation parameter, and several other data-model comparisons are presented. In addition, a discussion of OH(v) Einstein A coefficients is given in the appendix.

## 2. Kinetic Model Description

### 2.1. Mechanism

With the usual assumption that between 80 and 95 km altitudes OH(v) is produced from the H + $O_3$ reaction, the kinetic mechanism is given by

$$O + O_2 + M \rightarrow O_3 + M \quad M = N_2, O_2, O \qquad (1)$$

$$O_3 + H \rightarrow OH(v') + O_2 \quad v' \leq 9 \qquad (2)$$

$$OH(v') + O_2 \rightarrow OH(v'') + O_2 \qquad (3)$$

$$OH(v') + N_2 \rightarrow OH(v'') + N_2 \qquad (4)$$

$$OH(v') + O \rightarrow OH(v'') + O \qquad (5a)$$

$$\rightarrow H + O_2 \qquad (5b)$$

$$OH(v') \rightarrow OH(v'') + hv \qquad (6)$$

At higher altitudes, there is the possibility of one or more additional ozone formation reactions [*Allen*, 1986]. At nighttime the only sink for $O_3$ besides reaction (2) is the $O_3$ + O reaction, which is much slower. Therefore the rate of formation of OH can be equated with the rate of reaction (1).

Some investigators have proposed the $HO_2$ + O reaction as an additional source of OH(v). However, *Kaye* [1988] argued that it would be insignificant in the nightglow, and nearly all recent modeling studies have neglected it entirely. In any case, since the exothermicity of this reaction is insufficient to populate vibrational states above v=6, even if it were important for the lower levels it should make little contribution to the v = 5 thru 9 states that are the main focus of the present analysis. A potentially more important role for $HO_2$ is as an intermediate in OH(v) quenching, via

$$OH(v>6) + O_2 \rightarrow HO_2 + O \qquad (7)$$

$$HO_2 + O \rightarrow OH(v) + O_2 \qquad (8)$$

However, in the atmosphere this mechanism would be difficult if not impossible to distinguish from multiquantum vibrational quenching by $O_2$, and therefore it can be combined with reaction (3).

Following the usual approach, the above chemical kinetic equations are solved assuming that the intermediate species $O_3$ and OH(v) are in steady state; the net OH production rate equals the production rate of $O_3$ via reaction (1). While this treatment is not suitable for the study of gravity waves, it is more than adequate for the present investigation, in which time-averaged data are modeled, since (with the possible exception of O atoms near 80 km) the

average nighttime concentrations of the reagents in reaction (1) are reasonably stable.

**2.2. Kinetic Parameters**

The rate constants for reaction (1) are taken from the recommendations of *Steinfeld et al*. [1987]. The value for M = O has not been measured, but this contribution should be very small below 95 km.

The nascent distribution of OH(v) states (reaction (2)) has been measured by several investigators [*Charters et al.*, 1971; *Klenerman and Smith*, 1987; *Ohoyama et al*., 1985]. The Charters et al. values have been extrapolated to lower v using information theory by *Steinfeld et al*. [1987]. Renormalizing them to the Einstein coefficients of *Nelson et al.* [1990] yields the values in Table 1. Since these results are in good agreement with those of Klenerman and Smith, but are somewhat closer to the values of Oyohama et al. which have been adopted in many earlier modeling studies, they are used for the present work.

The quenching of OH(v) by O atoms (reactions (5a) and (5b)) is critical for establishing the populations of the $v < 5$ states but is much less important for the higher-v states examined in this study. The total removal rate for v = 1 has been measured as $1 \times 10^{-10}$ $cm^3$ (molecules $s)^{-1}$ at 300□ K [*Spencer and Glass*, 1977]. The branching ratio for chemical reaction versus vibrational relaxation has not been measured. While the magnitude of the rate constant, around 1/3 gas kinetic, might suggest the dominance of reaction, a recent study by *Dodd et al*. [1994] of nonthermal rotational emissions of OH suggests that the vibrational relaxation channel may be important. Similar to the v = 0 reaction rate [*DeMore et al*., 1990], the temperature dependence may be mildly negative. The rate constants for $v > 1$ are not known.

Given our present lack of knowledge of O + OH(v) relaxation for $v > 1$, in the present study a v-independent effective reactive quenching rate constant of $2 \times 10^{-10}$ $cm^3$ (molecules $s)^{-1}$ has been provisionally adopted based on simulations of v = 1 - 4 relative column populations. This value, twice the experimental value for quenching of v =1, is higher than typically assumed but not unreasonably so, considering the likelihood of a larger rate constant at high v. Since the effect of O atom quenching becomes increasingly important at higher altitudes, altitude-resolved data may provide valuable information on the quenching rate and mechanism.

We next consider the quenching of OH(v) by the major atmospheric gases (reactions (3) and (4)), which is important for $v \geq 5$. The rate constants may be specified by total removal rate constants and branching ratios for populating the lower v states. We first consider the total removal rate constants, $k_3(v)$ and $k_4(v)$. Accurate room-temperature values for $O_2$ have been measured for v = 1 to 6 by *Dodd et al*. [1991] and for v = 7 to 9 by Copeland and

coworkers [*Knutsen et al*., 1996; *Chalamala and Copeland*, 1993]. A partial set of measurements exists for $N_2$, which is a much slower quencher except near v = 8 where an $N_2$-OH vibrational resonance occurs (M. J. Dyer et al., unpublished data, 1997). For the present study the unpublished measurement by Dyer et al. for v = 8 has been adopted (see Table 1). For the remaining states, the values interpolated by *Makhlouf et al*. [1995] from several measurements have been chosen.

Since mesopause temperatures are typically around 190□ K, it is very important to consider the temperature dependence of the quenching rate constants, particularly for $O_2$. Preliminary work by M. J. Dyer et al. (unpublished data, 1997) has suggested that quenching of v = 10 by $O_2$ may decrease as the temperature is reduced from room temperature to 245° K but may rise again at 225° K.

Additional information on quenching rates at mesopause temperatures can be derived from the altitude dependence of the OH(v) nightglow. *McDade et al*. [1987] analyzed data from the ETON experiment, which measured the (8-3) band together with the O atom profile, and derived the ratio of the net quenching rate constant by $O_2$ and $N_2$, $k(8) = k_3(8) + 3.8k_4(8)$, to the v = 8 Einstein coefficient, A(8), for several different state-to-state relaxation models. Using the accurate value of A(8) from *Nelson et al*. [1990], their result yields $k(8) = (1.3 \pm 0.2) \times 10^{-11}$ cm$^3$ (molecules s)$^{-1}$ in the "sudden death" (SD) model limit. This value is within experimental error of the room temperature laboratory value, $k^{rt}(8) = k_3^{rt}(8) + 3.8k_4^{rt}(8) = (1.1 \pm 0.2) \times 10^{-11}$ cm$^3$ (molecules s)$^{-1}$. Since relaxation by $O_2$ dominates and the SD model gives a lower bound to the rate constant, at mesopause temperatures the collisional relaxation of v = 8 (and most likely the other v states as well) must be at least as fast as at room temperature.

In extracting quenching rate constants from the ETON profiles using some other state-to-state relaxation model, one can avoid a complete reanalysis of these data by using the approximate but simple method of matching vibrational state populations in the high $O_2 + N_2$ limit to the corresponding populations given by one of McDade's models. In this manner the net quenching rate constant for v = 8 can be related to the SD-derived value via

$$k(8) = k^{SD}(8)(1 + [f(9)/f(8)]\,[k(9,8)/k(9)]), \qquad (9)$$

where k(9,8) is the net rate constant for relaxation from v = 9 to v = 8, k(9) is the total removal rate constant for v = 9 by $O_2$ and $N_2$, f(8) and f(9) are the nascent state distribution fractions in v = 8 and 9, respectively (Table 1), and $k^{SD}(8)$ is the derived SD value of $1.3 \times 10^{-11}$ cm$^3$ (molecules s)$^{-1}$. The validity of (9) has been checked by verifying that for the most stressing, pure cascade case, in which the branching ratio k(9,8)/k(9) equals unity, the ratio of k(8) to $k^{SD}(8)$ predicted by (9) is similar to that obtained by *McDade et al*., [1987]

when the same values of f(8) and f(9) [from *Ohoyama et al*., 1985] are used.

If one assumes that any difference between the room-temperature value $k^{rt}(8)$ measured in the laboratory and the value k(8) inferred from the ETON data is due to temperature dependence, and also that the same dependence applies for all v and for both $N_2$ and $O_2$, then the laboratory rate constants are all scaled to mesopause temperatures using the factor, r, given by

$$r = k(v)/k^{rt}(v) = k(8)/k^{rt}(8) \qquad (10)$$

As is later shown, r is close to unity, so the precise scaling assumptions should not be critical to the analysis.

The most speculative yet important part of the OH vibrational relaxation problem concerns the branching ratios that define the state-to-state rate constants $k_3(v',v'')$ and $k_4(v',v'')$, which have not been measured. Some general characteristics of vibrational relaxation pathways in diatomic molecules have been established from experiments (e.g., cited by *Procaccia and Levine* [1975]) and molecular dynamics simulations [*Duff et al*., 1979; *Thompson*, 1992; *Wallis and Thompson*, 1992; *Duff and Sharma*, 1997]. Very slow relaxation tends to occur in single-quantum steps, as predicted by Schwartz-Slawsky-Hirschfeld theory. At the other extreme, efficient relaxation occurs when there is a stable collision complex, in which case the relaxation can be essentially statistical (all final states comparably populated) [*Duff and Sharma*, 1997]. In between these extremes, a blend of single-quantum and multiquantum relaxation is expected. All of these cases can be empirically modeled with an expression in which the relaxation probability varies exponentially with the vibrational energy gap or quantum number gap [*Procaccia and Levine*, 1975; *Duff et al.*, 1979; *Wallis and Thompson*, 1992]. Accordingly, low overall quenching probabilities are associated with extremely low multiquantum probabilities, while large overall quenching probabilities are associated with sizable multiquantum probabilities. This behavior is also consistent with viewing vibrational relaxation in terms of independent quantum-loss events.

Accordingly, for $N_2$, which is a very inefficient quencher of OH, single-quantum relaxation is assumed. On the other hand, for $O_2$, which is a more efficient quencher of OH and for which multiquantum relaxation is likely, a more sophisticated model is required. For the present study a simple and flexible expression incorporating exponential quantum-number-gap scaling has been chosen,

$$k_3(v',v'') = C[P_{v'}]^{\Delta v} \qquad (11)$$

where $\Delta v = v'-v''$, C is a constant for the entire system of rate constants, and $P_{v'}$ is a probability factor that is a function of v'. For a chosen value of C, one solves for the value of $P_{v'}$ for each v' such that the $k_3(v',v'')$ sum over v'' equals the total rate constant, $k_3(v')$. A small value of C yields large values of $P_{v'}$, hence substantial

multiquantum quenching, whereas a large value of C yields small values of $P_{v'}$, causing $\Delta v = 1$ cascade to dominate.

In support of (11), it may be shown to yield the same qualitative behavior as more complicated information theory-based expressions [*Procaccia and Levine*, 1975] for vibrational relaxation, and it is also quantitatively consistent with theoretical calculations of state-to-state relaxation rates for diatomic molecules including $H_2$ [*Duff et al*., 1979], OH [*Thompson*, 1982], and HF [*Wallis and Thompson*, 1992]. In particular, Figure 1 shows that (11) provides a very good match to classical trajectory calculations of the relaxation of HF(v) by CO at 300 ° K [*Wallis and Thompson*, 1992], a system which resembles OH + $O_2$ in terms of masses, dipole moments, and perhaps also in the ability to form a collision complex. In these calculations, the transition from single-quantum quenching at low v to multiquantum quenching at high v is clearly seen.

In summary, a complete set of state-to-state quenching rate constants for OH(v) has been defined in terms of known total removal rate constants and a single free parameter, C, that governs the degree of multiquantum relaxation by $O_2$. The value of C fixes the v = 9 branching ratio k(9,8)/k(9) and, via (9) and (10), the values of the mesospheric v = 8 rate constant and the temperature scaling factor, r. To determine C, a simulation of the vibrational distribution of the Meinel band intensities was performed, as described in section 3.1.

## 3. OH Nightglow Modeling

The nightglow modeling used the equations and rate constant values discussed in the previous section together with atmospheric species (O, $O_2$, and $N_2$) density and temperature profiles. The atmospheric profiles were taken from the MSISE-90 model [*Hedin*, 1991], except in modeling the data from the ETON experiment [*McDade et al*., 1987], where the measured O atom profile was used. O atom concentrations predicted by the MSIS-type models are generally believed to be reasonable averages, to within perhaps 30%, for given geophysical conditions. Estimates of mesopause temperature and major species ($N_2$, $O_2$) concentration uncertainties are on the order of 10 $K^o$ and 10%, respectively.

Einstein A coefficients are required in (6) to calculate the OH(v) populations as well as emission intensities. Several different sets of coefficients from the recent literature were investigated, as discussed in the appendix. The OH(v) populations are not very sensitive to the choice of coefficients; in particular, those of *Turnbull and Lowe* [1989] adjusted via (A1) and those of *Holtzclaw et al*. [1993] give virtually identical results. Furthermore, since the predicted relative intensities of bands at nearby wavelengths are insensitive to the

Einstein A coefficient set, relative intensity data are sufficient for evaluating the kinetic model.

### 3.1. Determination of the Multiquantum Relaxation Parameter from Zenith Radiance Simulations

As discussed in section 2, the C parameter defines the extent of multiquantum relaxation of OH(v) by $O_2$. For a given rate of relaxation of the highest-v states, the degree of multiquantum relaxation controls the feed rate into lower states and thus affects the relative populations. C can therefore be estimated from accurate column intensity measurements, such as have been made in ground-based experiments. By choosing bands at nearby wavelengths and considering the relative rather than the absolute intensities, the effects of both experimental intensity errors and Einstein A coefficient uncertainties are minimized.

In the current investigation, simulations were performed of the zenith (5 - 1), (6 - 2), (7 - 4), (8 - 3), and (9 - 4) relative band intensities which were measured by *Takahashi and Batista* [1981] over a several-year observation period. They found a small seasonal variation in the intensity ratios, with average values being close to that for spring 1977. Similar intensity ratios were also measured in the photographic spectrum of *Krassovsky et al*. [1962].

The simulations of the Takahashi and Batista measurements were performed using an MSISE-90 model atmosphere for typical spring nighttime conditions at the measurement location. The ratios of the predicted to observed radiances were taken and divided by their mean; the rms difference of the result from unity represents the average relative intensity error for these bands.

The relative intensity error is shown as a function of the trial value of C/r in Figure 2. Using either of two different Einstein A coefficient sets (from *Holtzclaw et al*. [1993] and *Turnbull and Lowe* [1989], adjusted via (A1); see the appendix), the best fit value of C/r is approximately 3 x $10^{-12}$ $cm^3$ (molecules $s)^{-1}$. With that value, the RMS errors are very low, around 7 to 8%, which is comparable to the measurement uncertainty and variability. Given the additional uncertainties in the OH(v) nascent distribution, the total quenching rate constants, and the shape of the O atom profile, it is difficult to assign error limits to C/r; a rough estimate is that it is accurate to within better than a factor of 2.

For C/r values close to the best fit, r is around 1.4. The analysis was later repeated using the experimental upper limits on $k_3^{rt}(8)$ and $k_4^{rt}(8)$; this analysis will be referred to as model 2. The same best fit C/r value is obtained, but r is reduced to 1.2. Since the latter value is not significantly greater than unity, one cannot definitively conclude that the mesopause rate constants are larger than the room-temperature values. Further experiments are needed to settle this issue.

The OH(v) radiance data and model simulations are compared in Figure 3 for the original model, for model 2, and for the limiting cases of single-quantum cascade (C □ □) and sudden death (C □ 0). For either the original model or model 2 and either set of Einstein coefficients, the absolute radiance agreement is within 25% or better for all v, which is remarkably good considering all the possible sources of uncertainty. In contrast, the cascade and sudden-death models both give poor results, with errors of up to factors of 2.

The OH(v) + $O_2$ relaxation parameters C and $P_v$ obtained in this work are summarized in Table 2. State-to-state rate constants calculated from these parameters appear in Table 3. According to these results, at v = 9 all product vibrational states are equally likely ($P_v$ is close to unity), whereas at low v the relaxation is almost entirely single quantum ($P_v$ is much less than unity).

### 3.2. Additional Data/Model Comparisons and Predicted Altitude Profiles

Several additional data-model comparisons were carried out to verify the present model.

*McDade and Llewellyn* [1987] have tabulated mean relative column densities for OH(v) from v = 1 to 9 from several sets of measurements. Their values are compared with the results from the Takahashi and Batista data simulation in Figure 4. Both the basic model and Model 2 give very similar overall agreement, although for model 2 the overestimation at v = 7 is slightly increased. Using a OH(7) + $N_2$ relaxation rate constant that is somewhat larger than the Table 1 estimate (but below the upper limit of 6 x $10^{-13}$ $cm^3$ (molecules $s)^{-1}$ from Knutsen et al. (1996)) would eliminate the v = 7 error.

Figure 5 shows a comparison of a model calculation and the (8 - 3) band altitude profile measured in the ETON experiment. Here, the (8 - 3) Einstein A coefficient was chosen to match the integrated intensity. The model gives very good agreement with the altitude profile shape, as expected from the fact that the model value of k(8) was indirectly derived from these data.

A similar (8 - 3) band measurement has been reported by *Takahashi et al*. [1996]. Using their O atom profile above 86 km, which was obtained indirectly from $O_2$ atmospheric band emission, the present model yields excellent agreement with their (8 - 3) band profile shape. With the Holtzclaw et al. A coefficient the absolute intensity agreement is within 10%. With the (A1) A coefficient, which matches the ETON data, the predicted intensity is too low by 30%; however, this is still within the range of experimental errors.

We are unaware of other OH(v) altitude profile measurements that are free from optical contamination and for which at least the atomic oxygen concentration is known. Predicted altitude profiles from the simulation of the *Takahashi and Batista* [1981] data are shown in Figure 6. These profiles provide a good average

representation of available measurements from rocket experiments (see *Baker and Stair* [1988], for a comprehensive survey). At the highest altitudes, the OH(v) distribution is predicted to be very flat. However, there it is sensitive to quenching by O atoms, and it would be less flat if the quenching were slower, had a positive v dependence, or were mainly nonreactive.

According to the prediction in Figure 6, the altitude of the peak OH(v) concentrations (and hence emissions) is given approximately by (83 + 0.7v) km. The v dependence is larger than in most previous models because fast, reactive quenching by O atoms has been assumed. Simultaneous airglow measurements by *Mende et al*. [1993] found no significant differences in the peak altitudes for v = 6 through 8 emissions. However, the data of *Lopez-Moreno et al*. [1987], which cover mainly v = 3 through 6, and a preliminary analysis of data from the large number of experiments in the *Baker and Stair* [1988] compilation both suggest an average altitude increase of about 0.5 km per vibrational quantum, in reasonable agreement with the present model considering the uncertainties in the O atom quenching mechanism.

Some preliminary comparisons of predicted vibrational state distributions with data from the limb-viewing CIRRIS-1A experiment [*Dodd et al*., 1994] have also been performed. The comparisons are promising, but the analysis is complicated by the sizable vertical footprints of the detectors, by tangent height uncertainties, and by the lack of a measured O atom profile, so that further investigation is required.

## 4. Summary and Conclusions

An improved state-to-state kinetic model for the Meinel bands of OH has been constructed from rate constants and Einstein A coefficients derived in recent laboratory experiments. Using a semi-empirical parameterization of OH(v) quenching by $O_2$, the nightglow altitude dependence and OH(v) absolute radiances have been modeled to within the accuracies of the atmospheric constituent concentrations and radiometric calibrations, and the multiquantum nature of the quenching has been characterized. Possible errors due to Einstein coefficient, radiance, and atmospheric constituent uncertainties have been minimized by using only relative intensities to derive the model parameters. While there are still substantial uncertainties in the model rate constants that reflect necessary simplifying assumptions, the following results and conclusions of this study are well supported:

1. The net rates of OH (v = 5 - 9) relaxation by the major atmospheric species, $O_2$ and $N_2$, at the mesopause are similar to those measured in the laboratory at room temperature.

2. Vibrational relaxation by $O_2$ is multiquantum at the high v levels but single-quantum at the low v levels, as has been proposed by other investigators.

3. Very good absolute agreement (within 30% or better) is obtained between several different sets of simulated and observed $\Delta v = 5$ nightglow radiances using the Einstein A coefficients calculated by *Holtzclaw et al*. [1993], which are based on the *Nelson et al*. [1990] dipole moment function. This result strongly supports the use of the Nelson et al. dipole moment function for Meinel band modeling.

Additional experimental investigations are needed to quantitatively test this model and improve our understanding of OH(v) kinetics in the atmosphere. In particular, further measurements are needed of (1) the products and rate constants for OH(v) removal by O atoms, and (2) rate constants for OH(v) quenching by $O_2$ at mesopause temperatures.

For the high-v (v= 7 - 9) emissions, the present model and those of *McDade et al.* [1987] and *McDade and Llewellyn* [1987] are very similar in their predictions and uncertainties; thus, similar $O + O_2 + M$ rate profiles would be derived from high-v data using any of these models. The greatest uncertainties are in the low-v emissions. The present model predicts these emissions to occur several km below the predictions of the McDade models, so that recombination rate profiles derived from low-v data would be several km higher. An analysis of simultaneous measurements of high-v and low-v emission profiles would provide a valuable consistency check for all of the models.

## Appendix: OH(v) Einstein Coefficients

The most accurate available Einstein A coefficients for the fundamental and low-overtone bands of OH are believed to be those derived by *Nelson et al*. [1990] from laboratory measurements of $\Delta v = 1$ and $\Delta v = 2$ transitions. For the higher overtones, the available calculations show strong disagreements. In general, the calculations of *Turnbull and Lowe* [1989] predict the strongest overtones and the calculations of *Langhoff et al*. [1986], which agree reasonably with Nelson's for $\Delta v$ of up to 3, predict the weakest. The discrepancy for the $\Delta v = 5$ overtones is around a factor of four among these calculations. Another set of values commonly used for nightglow modeling are the relative Einstein coefficients of *Murphy* [1971]. When normalized to the Nelson et al. radiative lifetimes, Murphy's results give intermediate overtone intensities.

In principle, the method used by Turnbull and Lowe should have given accurate results, since it was based on fitting to relative band intensities measured in nightglow spectra. However, an inaccurate intensity calibration in one or more of the spectra they used would have led to a systematic error as a function of the band center

frequency. The ratio of corresponding line strengths from Turnbull and Lowe and from Nelson et al. is plotted in Figure 7. The smooth, monotonic dependence strongly suggests that intensity calibration error is indeed responsible for the differences between the Turnbull and Lowe and Nelson et al. values.

The ratios in Figure 7 define a calibration "correction" curve that can be used to convert Turnbull and Lowe's thermally averaged Einstein A coefficients, denoted $A_{TL}$, into values consistent with Nelson et al.'s. The smooth Gaussian curve shown is a least squares fit based on Nelson et al.'s A values for $\Delta v$ of up to 3 plus the value of A(8-3) which gives the best agreement between the absolute intensities measured in the ETON experiment and the present model simulation, shown in Figure 5. The curve is given by

$$\ln(A/A_{TL}) = -0.228 + 9.8\times10^{-6}v - 4.6\times10^{-9}v^2, \qquad \text{(A1)}$$

where v is the band center frequency in $cm^{-1}$. The A coefficients obtained by applying (A1) to Turnbull and Lowe's results should be accurate to better than ±10% for the $\Delta v$ = 1 to 3 transitions and ±25% for the $\Delta v$ = 4 and 5 transitions.

More recently, *Holtzclaw et al*. [1993] used Nelson's dipole moment function to extrapolate A values for up to $\Delta v$ = 5 transitions. This calculation may provide the best available theoretical values for $\Delta v$ = 4 and 5, even though (as Nelson et al. had pointed out) the dipole moment function is deficient in high derivatives that can potentially affect these transitions. The ratio of the Turnbull and Lowe to the Holtzclaw et al. Einstein coefficients is shown in Figure 7 for $\Delta v$ = 4 and 5 bands. The difference versus (A1) is about 20% for A(8 - 3), which is well within the accuracy of the estimate from the ETON data.

Consistent with the above analysis, the *Turnbull and Lowe, Holtzclaw et al*. and (A1)-"corrected" Einstein coefficient ratios for bands with nearly the same center frequencies are virtually identical, even for the high-overtone bands. For example, for the (9 - 4) and (5 - 1) bands the three ratios agree to within 5%.

For completeness, some additional $A/A_{TL}$ values for high-overtone transitions are plotted in Figure 7. Values for the (8 - 3) and (9 - 3) bands based on the work of *Murphy* [1971] are shown, and are seen to be in good agreement with (A1). In laboratory measurements by *Finlayson-Pitts and Kleindienst* [1981], vibrational quenching rates were derived as a function of the assumed (9 - 3) band Einstein coefficient. Using this functional relationship [see *McDade and Llewellyn*, 1987] and the rate constants for quenching by $CO_2$ and $O_2$ measured by *Chalamala et al.* [1993], an Einstein coefficient of $0.3 \pm 0.1\ s^{-1}$ ($A/A_{TL} = 0.48 \pm 0.16$) is inferred. This value lies somewhat above the (A1) curve but is fairly close to an extrapolation of the $A/A_{TL}$ values from Holtzclaw et al.

**Acknowledgments.** The author is very grateful to D. R. Smith (Phillips Laboratory, Hanscom AFB) for his encouragement and oversight of this investigation. He also thanks J. Duff and L. Bernstein (Spectral Sciences, Inc.) for review of the manuscript, J. Dodd (USU Stewart Radiance Laboratory, Bedford Massachusetts), I. McDade (Herzberg Institute), W. Blumberg and S. Lipson (Phillips Laboratory) for stimulating discussions and constructive suggestions, and K. Holtzclaw (Physical Sciences Inc., Andover Massachusetts) and R. Copeland (SRI) for sharing research results prior to publication. This work was supported by the U.S. Air Force under contract F19628-91-C-0083 and by Spectral Sciences, Inc.

## 5. References

Baker, D. J., and A. T. Stair Jr., Rocket measurements of the altitude distributions of the hydroxyl airglow, *Phys. Scri*., *37*, 611, 1988.

Chalamala, B. R., and R. A. Copeland, Collision dynamics of OH($X^2\pi$,v=9), *J. Chem. Phys., 99*, 5807, 1993.

Charters, P. E., R. G. McDonald, and J. C. Polanyi, Formation of vibratonally excited OH by the reaction H + $O_3$, *Appl. Opt., 10*, 1747, 1971.

DeMore, W. B., S. P. Sander, D. M. Golden, M. J. Molina, R. F. Hampson, M. J. Kurylo, C. J. Howard, and A. R. Ravishankara, Chemical kinetics and photochemical data for use in stratospheric modeling, *JPL Publ.* 90-1, 217 pp., Jet Propul. Lab., Calif. Inst. Technol., Pasadena, 1990.

Dodd, J. A., S. J. Lipson, and W. A. M. Blumberg, Formation and vibrational relaxation of OH ($X^2\pi_i$,v) by $O_2$ and $CO_2$, *J. Chem. Phys.*, *95*, 5752, 1991.

Dodd, J. A., S. J. Lipson, J. R. Lowell, P. S. Armstrong, W. A. M. Blumberg, R. M. Nadile, S. M. Adler-Golden, W. J. Marinelli, K. W. Holtzclaw, and B. D. Green, Analysis of hydroxyl earthlimb airglow emissions: Kinetic model for state-to-state dynamics of OH(v,n), *J. Geophys. Res.*, *99*, 3559, 1994.

Duff, J. W., and R. D. Sharma, Quasiclassical trajectory study of NO vibrational relaxation by collisions with atomic oxygen, *J. Chem. Soc. Faraday Trans.*, *93*, in press, 1997.

Duff, J. W., N. C. Blais, and D. G. Truhlar, Monte Carlo trajectory study of Ar + $H_2$ collisions: Thermally averaged vibrational transition rates at 4500$^o$ K, *J. Chem. Phys.*, *71*, 11, 1979.

Finlayson-Pitts, B. J., and T. E. Kleindienst, The reaction of hydrogen atoms with ozone as a source of vibrationally excited $OH(X^2\pi_i)_{v=9}$ for kinetic studies, *J. Chem. Phys., 74*, 5643, 1981.

Hedin, A. E., Extension of the MSIS thermosphere model into the middle and lower atmosphere, *J. Geophys. Res., 96*, 1159, 1991.

Holtzclaw, K. W., J. C. Person, and B. D. Green, Einstein coefficients for emission from high rotational states of the OH($X^2\pi$) radical, *J. Quant. Spectrosc. Radiat. Transfer*, *49*, 223, 1993.

Kaye, J. A., On the possible role of the reaction O + $HO_2$ □ OH + $O_2$ in OH airglow, *J. Geophys. Res., 93*, 285, 1988.

Klenerman, D., and I. W. M. Smith, Infrared chemiluminescence studies using a SISAM spectrometer, *J. Chem. Soc. Faraday Trans*. *2*, *83*, 229, 1987.

Knutsen, K., M. J. Dyer, and R. A. Copeland, Collisional removal of OH ($X^2\pi$, $v$=7) by $O_2$, $N_2$, $CO_2$, and $N_2O$, *J. Chem. Phys.*, *104*, 5798, 1996.

Krassovsky, V. I., N. N. Shefov, and V. I. Yarin, Atlas of the airglow spectrum 3000-12,400 angstroms, *Planet. Space. Sci., 9*, 883, 1962.

Langhoff, S. R., H-J. Werner, and P. Rosmus, Theoretical transition probabilities for the OH Meinel system, *J. Molec. Spectrosc., 118*, 507, 1986.

Lopez-Moreno, J. J., R. Rodrigo, F. Moreno, M. Lopez-Puertas, and A. Molina, Altitude distribution of vibrationally exited states of atmospheric hydroxyl at levels $v$ = 2 to $v$ = 7, *Planet. Space Sci., 35,* 1029, 1987.

Makhlouf, U. B., R. H. Picard, and J. R. Winick, Photochemical-dynamical modeling of the measured response of airglow to gravity waves, *J. Geophys. Res., 100*, 11289, 1995.

McDade, I. C., The altitude dependence of the OH($X^2\pi$) vibrational distribution in the nightglow: Some model expectations, *Planet. Space. Sci.*, *39*, 1049, 1991.

McDade I. C., and E. J. Llewellyn, Kinetic parameters related to sources and sinks of vibrationally excited OH in the nightglow, *J. Geophys. Res.*, *92*, 7643, 1987.

McDade, I. C., E. J. Llewellyn, D. P. Murtagh, and R. G. H. Greer, ETON 5: Simultaneous rocket measurements of the OH Meinel $\Delta v$=2 sequence and (8,3) band emission profiles in the nightglow, *Planet. Space. Sci.*, *35*, 1137, 1987.

Mende, S. B., G. R. Swenson, S. P. Geller, R. A. Viereck, E. Murad, and C. P. Pike, Limb view spectrum of the earth's airglow, *J. Geophys. Res., 98*, 19, 1993.

Murphy, R. E., Infrared emission of OH in the fundamental and first overtone bands, *J. Chem. Phys., 54*, 4852, 1971.

Nelson Jr., D. D., A. Schiffman, D. J. Nesbitt, J. J. Orlando, and J. B. Burkholder, H + $O_3$ Fourier-transform infrared emission and laser absorption studies of OH($X^2\pi$) radical: An experimental dipole moment function and state-to-state Einstein A coefficients, *J. Chem. Phys., 93*, 7003, 1990.

Ohoyama, H., T. Kasai, Y. Yoshimura, H. Kimura, and K. Kuwata, Initial distribution of vibration of the OH radicals produced in the H + $O_3$ □ OH($X^2\pi_{1/2,3/2}$) + $O_2$ reaction: Chemiluminescence by a crossed beam technique, *Chem. Phys. Lett*., *118*, 263, 1985.

Pendleton Jr., W., P. Espy, D. J. Baker, A. Steed, M. Fetrow, and K. Henriksen, Evidence for nonlocal thermodynamic equilibrium rotation in the OH nightglow, *J. Geophys. Res.*, *54*, 505, 1989.

Procaccia, I., and R. D. Levine, Vibrational energy transfer in molecular collisions: An information theoretic analysis and synthesis, *J. Chem. Phys*., *62*, 2496, 1975.

Shalashilin, D. V., A. V. Michtchenko, S. Ya. Umanskii, and Y. M. Gershenzon, Simulation of effective vibrational-translational energy exchange in collisions of vibrationally excited OH with $O_2$ on the model

potential energy surface. Can the relaxation of OH(v) be one-quantum for low and multiquantum for high v? *J. Phys. Chem.*, *99,* 11627, 1995.

Smith, D. R., W. A. M. Blumberg, R. M. Nadile, S. J. Lipson, E. R. Huppi, N. B. Wheeler, and J. A. Dodd, Observation of high-N hydroxyl pure rotation lines in atmospheric emission spectra by the CIRRIS 1A space shuttle experiment, *Geophys. Res. Lett.*, *19*, 593, 1992.

Spencer J. E., and G. P. Glass, Some reactions of OH(v=1), *Int. J. Chem. Kinetics, 9*, 111, 1977.

Steinfeld, J. I., S. M. Adler-Golden, and J. W. Gallagher, Critical survey of data on the spectroscopy and kinetics of ozone in the mesosphere and thermosphere, *J. Phys. Chem. Ref. Data, 16*, 911, 1987.

Takahashi, H., and P. P. Batista, Simultaneous Measurements of OH(9,4), (8,3), (7,2), (6,2), and (5,1) Bands in the Nightglow, *J. Geophys. Res.*, *86*, 5632, 1981.

Takahashi, H., M.L. Stella, B.R. Clemesha, and D.M. Simonich, Atomic hydrogen and ozone concentrations derived from simultaneous lidar and rocket airglow measurements in the equatorial region, *J. Geophys. Res.*, *101*, 4033, 1996.

Tarasick D. W., and G. G. Shepherd, Effects of gravity waves on complex airglow chemistries. 2. OH emission, *J. Geophys. Res.*, *97*, 3195, 1992.

Thomas, R. J., Atomic hydrogen and oxygen density in the mesopause region: Global and seasonal variations deduced from Solar Mesosphere Explorer near-infrared emissions," *J. Geophys. Res., 95*, 16457, 1990.

Thompson, D. L., Quasiclassical trajectory state-to-state cross sections for energy transfer in Ar + OH(v=9, J=0, 4, and 8) collisions, *Chem. Phys. Lett., 92*, 383 (1982); Vibrational-rotational-translational energy transfer in Ar + OH. Quasiclassical trajectory state-to-state cross sections, *J. Phys. Chem., 86*, 2538, 1982.

Turnbull D. N., and R. P. Lowe, New hydroxyl transition probabilities and their importance in airglow studies, *Planet. Space. Sci.*, *37*, 723, 1989.

Wallis E. P., and D. L. Thompson, Quasiclassical trajectory study of HF(v) by CO, *J. Chem. Phys.*, *97*, 4929, 1992.

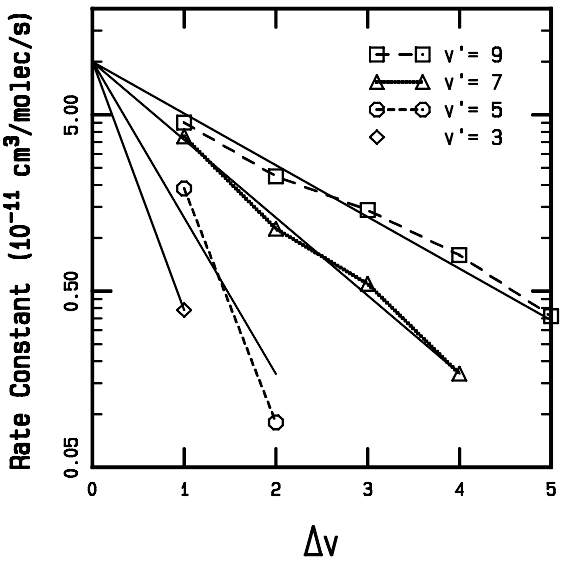


**Figure 1.** Comparison of parameterization (11) (solid lines) with trajectory calculations [*Wallis and Thompson*, 1992] of the state-to-state rate constants for relaxation of HF(v) by CO.

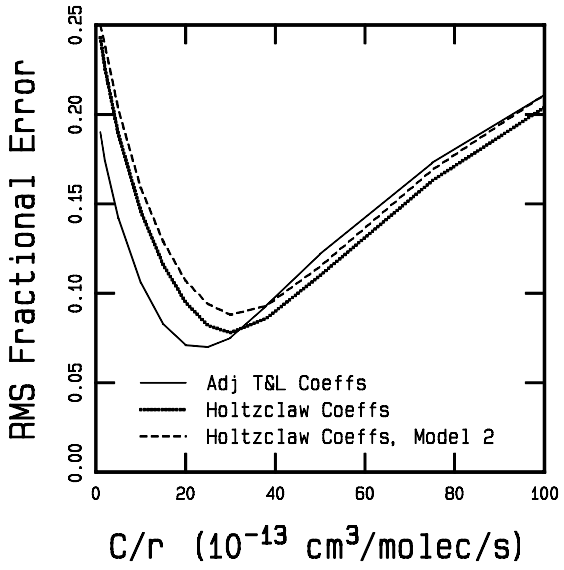


**Figure 2.** Data [*Takahashi and Batista*, 1981] versus model agreement for the OH (9 - 4), (8 - 3), (7 - 2), (6 - 2), and (5 - 1) band relative zenith radiances as a function of the relaxation parameter C.

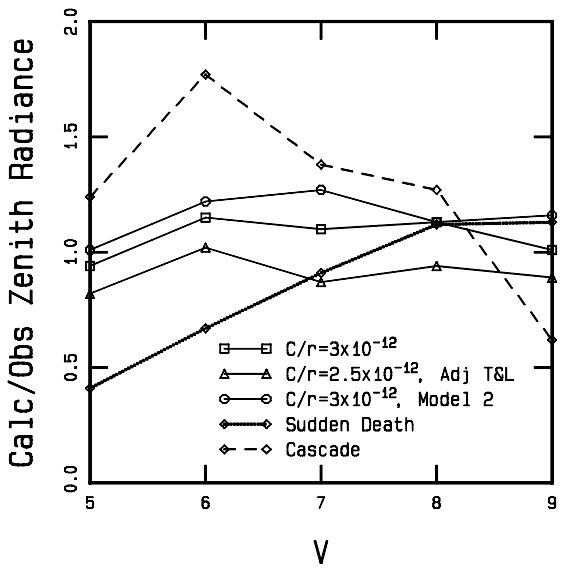


**Figure 3.** Absolute OH(v) radiances relative to the *Takahashi and Batista* [1981] data as predicted by different quenching models. Einstein coefficients from *Holtzclaw et al.* [1993] were used unless otherwise noted.

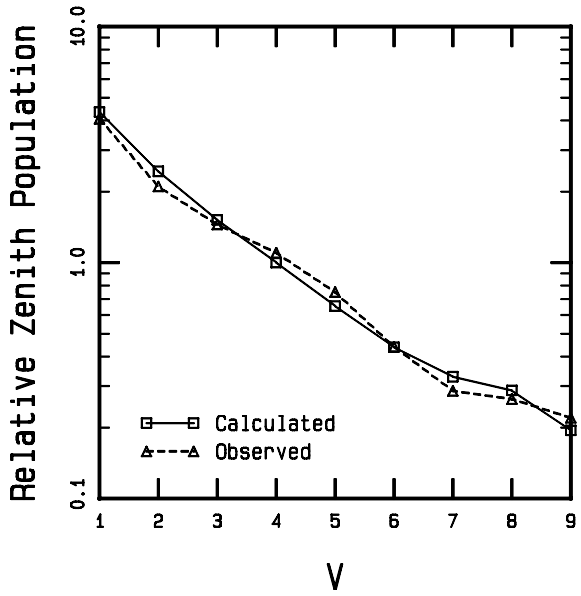


**Figure 4.** Comparison of predicted zenith column OH(v) populations with average nightglow estimates from *McDade and Llewelyn* [1987].

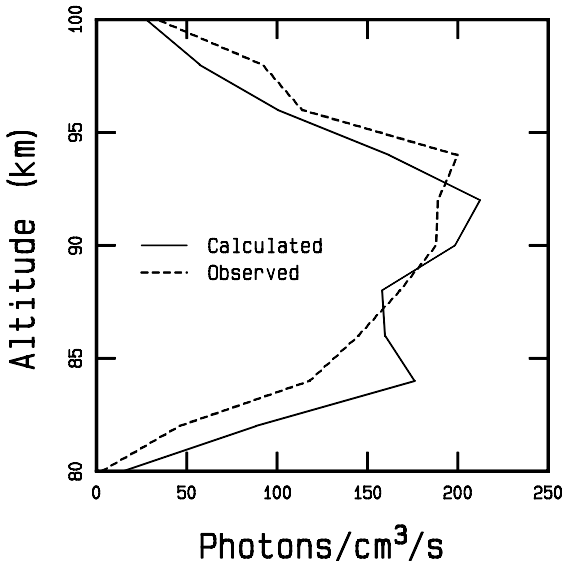


**Figure 5.** Simulation of the (8 - 3) band profile from the ETON experiment. $A(8 - 3) = 0.78\ s^{-1}$ in the model calculation.

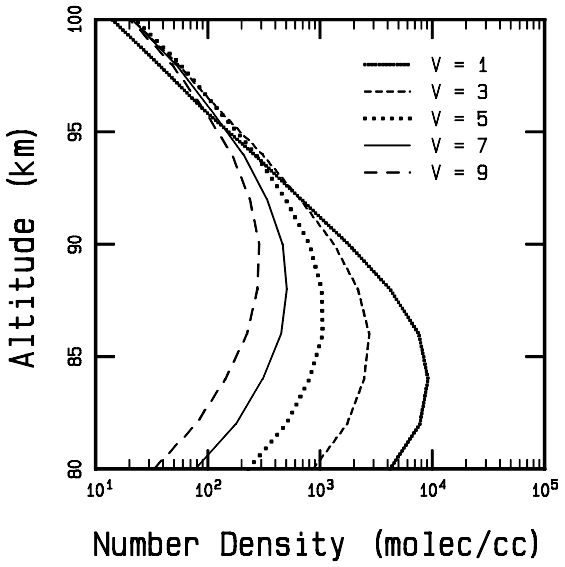


**Figure 6.** Predicted OH(v) altitude profiles from the Figure 3 calculation (basic model).

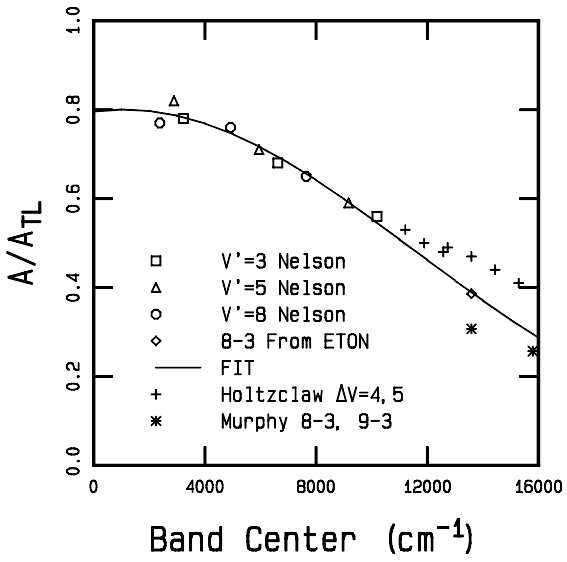


**Figure 7.** Comparison of Einstein A coefficients from *Turnbull and Lowe* [1989] and other authors.

**Table 1.** Room-Temperature Rate Constants for OH(v) Quenching by $O_2$ ($k_3$) and $N_2$ ($k_4$) and the Nascent Distribution for Formation ($f_v$)

| v | $10^{13}k_3(v)$, $cm^3$ (molecules $s)^{-1}$ | $10^{13}k_4(v)$, $cm^3$ (molecules $s)^{-1}$ | $f_v = k_2(v)/k_2$ |
|---|---|---|---|
| 1 | 1.3 | 0.06 | 0 |
| 2 | 2.7 | 0.10 | 0 |
| 3 | 5.2 | 0.17 | 0 |
| 4 | 8.8 | 0.30 | 0 |
| 5 | 17 | 0.52 | 0.01 |
| 6 | 30 | 0.91 | 0.03 |
| 7 | 70 | 1.6 | 0.15 |
| 8 | 80 (90) | 7 (11) | 0.34 |
| 9 | 200 | 4.8 | 0.47 |

Upper limit values used for model 2 are shown in parentheses.

**Table 2.** Values for OH(v) + $O_2$ Rate Constant Equation (11)

$C = 4.4\ (3.5) \times 10^{-12}\ cm^3$ (molecules $s)^{-1}$

| v | $P_v$ |
|---|---|
| 1 | 0.043 |
| 2 | 0.083 |
| 3 | 0.15 |
| 4 | 0.23 |
| 5 | 0.36 |
| 6 | 0.50 |
| 7 | 0.72 |
| 8 | 0.75 (0.78) |
| 9 | 0.95 |

Model 2 values are shown in parentheses.

**Table 3.** State-to-State Quenching Rate Constants $k_3(v',v'')$ Calculated From the Table 2 Values (Model 1)

| | v@ | | | | | | | | |
|---|---|---|---|---|---|---|---|---|---|
| | 0 | 1 | 2 | 3 | 4 | 5 | 6 | 7 | 8 |
| v'=1 | 2 | | | | | | | | |
| v'=2 | 0 | 4 | | | | | | | |
| v'=3 | 0 | 1 | 7 | | | | | | |
| v'=4 | 0 | 1 | 2 | 10 | | | | | |
| v'=5 | 0 | 1 | 2 | 6 | 16 | | | | |
| v'=6 | 1 | 1 | 3 | 6 | 11 | 22 | | | |
| v'=7 | 4 | 6 | 9 | 12 | 16 | 23 | 32 | | |
| v'=8 | 4 | 6 | 8 | 10 | 14 | 19 | 25 | 33 | |
| v'=9 | 28 | 29 | 31 | 32 | 34 | 36 | 38 | 40 | 42 |

In units of $10^{-13}$ $cm^3$ $(molecules\ s)^{-1}$.